

LETTER TO THE EDITOR

Unveiling the circumstellar environment towards a massive young stellar object

S. Paron^{1,2}, C. Fariña³, and M. E. Ortega¹

¹ Instituto de Astronomía y Física del Espacio (IAFE), CC 67, Suc. 28, 1428 Buenos Aires, Argentina
e-mail: sparon@iafe.uba.ar, mortega@iafe.uba.ar

² FADU and CBC, Universidad de Buenos Aires, Argentina

³ Isaac Newton Group of Telescopes, E-38700, La Palma, Spain
e-mail: cf@ing.iac.es

Received <date>; Accepted <date>

ABSTRACT

Aims. As a continuation of a previous work, in which we found strong evidence of massive molecular outflows towards a massive star forming site, we present a new study of this region based on very high angular resolution observations with the aim of discovering the outflow driven mechanism.

Methods. Using near-IR data acquired with Gemini-NIRI at the broad *H*- and *Ks*-bands, we study a region of 22''×22'' around the UCH_{II} region G045.47+0.05, a massive star forming site at the distance of about 8 kpc. To image the source with the highest spatial resolution possible we employed the adaptative optic system ALTAIR, achieving an angular resolution of about 0''.15.

Results. We discovered a cone-like shape nebula with an opening angle of about 90° extending eastwards the IR source 2MASS J19142564+1109283, a very likely MYSO. This morphology suggests a cavity that was cleared in the circumstellar material and its emission may arise from scattered continuum light, warm dust, and likely emission lines from shock-excited gas. The nebula, presenting arc-like features, is connected with the IR source through a jet-like structure, which is aligned with the blue shifted CO outflow found in a previous study. The near-IR structure lies ~3'' north of the radio continuum emission, revealing that it is not spatially coincident with the UCH_{II} region. The observed morphology and structure of the near-IR nebula strongly suggest the presence of a precessing jet. In this study we have resolved the circumstellar ambient (in scale of a thousand A.U.) of a distant MYSO, indeed one of the farthest cases.

Key words. Stars: formation – ISM: jets and outflows – (ISM): H_{II} regions

1. Introduction

The formation of high-mass stars plays a very important role in the evolution and dynamics of the Galaxy. Despite the high impact that they have on the environment, the physical processes involved in their formation are less understood than those of their low-mass counterpart. The birth of a massive star is a violent event, that produces intense extreme ultraviolet radiation ionizing the surroundings (e.g. Hester & Desch 2005; Peters et al. 2010). The formation of a massive star also produces jets and massive molecular outflows (e.g. Wu et al. 2004; Vaidya et al. 2011) which may contribute to the removal of excess angular momentum from accreted matter and to disperse infalling circumstellar envelopes (Reipurth & Bally 2001; Preibisch et al. 2003). Such a phenomenon can take place even when the object has reached the ultracompact H_{II} (UCH_{II}) region stage (Hunter et al. 1997; Qin et al. 2008). Taking into account that high-mass stars generally do not form in isolation but in dense clusters and that the massive star formation sites are located at far distances, very high angular resolution imaging is required to reveal the morphologies of their circumstellar ambient.

The UCH_{II} region G045.47+0.05 (hereafter G45.47) is located towards the eastern border of the extended H_{II} region G45L (Paron et al. 2009) and deeply embedded in a dense and dark

molecular cloud. Figure 1 displays a three-color *Spitzer*-IRAC image of a large field where G45.47 is located and the white box indicates its position. The IRAC data were extracted from the GLIMPSE Survey (Benjamin et al. 2003). G45.47 is included in the extensive study of UCH_{II} regions of Wood & Churchwell (1989), who adopted the distance of 9.7 kpc for it. According to Paron et al. (2009), the H_{II} region G45L is located at a distance of about 8 kpc, same as the UCH_{II} region complex G45.45+0.06 (Kuchar & Bania 1994), which is the brightest structure in Fig. 1. By considering that all these sources belong to a same complex, Ortega et al. (2012) adopted the distance of 8.3 kpc for G45.47. However, following Araya et al. (2002), distances down to 6 kpc cannot be excluded for this source. Class II CH₃OH maser emission at 6.6 GHz was detected towards G45.47 (Caswell et al. 1995) with a central velocity of 56 km s⁻¹, which is in agreement with the systemic velocities of the H_{II} region complex and the related molecular cloud. It is known that such a maser is radiatively pumped by IR emission from the warm dust associated with massive young stellar objects (MYSOs). Indeed, in a previous study, Cesaroni et al. (1992) using NH₃ lines observations found evidence of collapse towards G45.47. Based on high-angular resolution (~5'') molecular line observations, Wilner et al. (1996) identified several HCO⁺ J=1–0 clumps suggesting that G45.47 is in the early stages of forming an OB cluster. G45.47 is associated with an extended source seen at 4.5 μm in *Spitzer*-IRAC images, the “ex-

Send offprint requests to: S. Paron

tended green object” EGO G45.47+0.05, which was cataloged by Cyganowski et al. (2008) as a “likely” MYSO outflow candidate. Recently, Ortega et al. (2012) using intermediate angular resolution observations from several molecular transitions, characterized the dense molecular clump where G45.47 is embedded and found strong evidence of outflow activity in the region.

In this study, we report the results obtained from near-IR observations performed with Gemini-NIRI with high-angular resolution towards G45.47.

2. Observations and data reduction

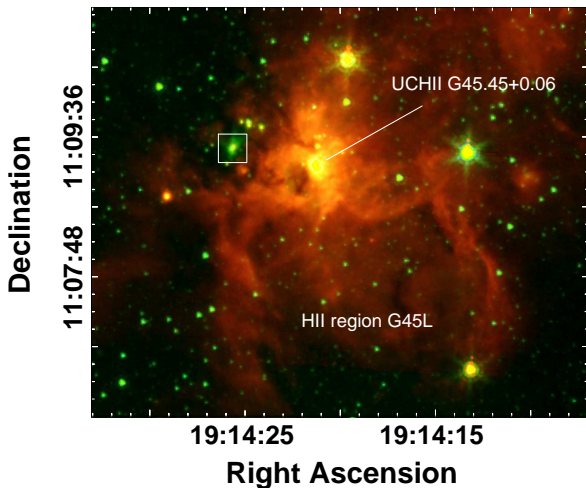


Fig. 1. Three-color *Spitzer*-IRAC image of a large field where the UCH_{II} region G45.47 is located ($8\ \mu\text{m}$ in red, $4.5\ \mu\text{m}$ in green, and $3.5\ \mu\text{m}$ in blue). The white box indicates the field observed with Gemini-NIRI and G45.47 is the extended green source within it.

In this study we analyzed the *H* and *K_s* broad-band images of the UCH_{II} region G45.47 acquired with NIRI (Hodapp et al. 2003) at Gemini-North. The observations were carried out during April and June 2012 in queue mode (Program GN-2012A-Q-20). NIRI was used with the *f*/32 camera that provides a plate scale of $0''.022\ \text{pix}^{-1}$ in a field of view of $22''\times 22''$. The white box in Fig. 1 represents the field observed with NIRI centered at RA = $19^{\text{h}}14^{\text{m}}25.6\text{s}$, dec. = $+11^{\circ}09'28.5''$, J2000. To image the source with the highest spatial resolution possible, NIRI was used together with the Gemini facility adaptive optics (AO) system, ALTAIR (Herriot et al. 2000; Boccas et al. 2006). For the AO the laser guide star system (LGS) was necessary (with a natural guide star only for tip/tilt correction) because G45.47 is deeply embedded in a dense molecular clump with high extinction and it was not possible to find a nearby star that fulfill the AO brightness requirement in the optical V-band. The available natural tip/tilt star was offset from the UCH_{II} region as well and was relatively faint which resulted in a slight elongation of the PSF, noticeable mainly in the *H*-band. The images in both, *H*- and *K_s*-bands were performed using a dither pattern with offsets to sky fields. The images were reduced using standard procedures for near-infrared (near-IR) imaging provided by the Gemini Observatory through the IRAF-NIRI package. The effective seeing was $\sim 0''.15$ (as measured as the FWHM of point sources in the field of the final co-added images). After excluding several individual frames with anomalous electronic noise and with evident bad-quality PSFs, the effective exposure times of the final co-added images were 50 s and 120 s for the *K_s*- and *H*-band,

respectively. The signal to noise of the extended emission is ~ 20 for the *K_s*-band and ~ 7 for the *H*-band. The absolute astrometry in NIRI images was performed using three near-IR stars in the field from the 2MASS Point Source Catalog, fortunately the three stars were well distributed in the field allowing a good astrometrical solution.

3. Results and discussion

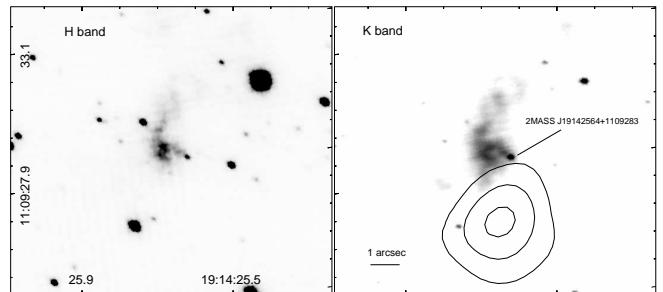


Fig. 2. Left: *H*-band emission towards G45.47. Right: same field displaying the *K_s*-band emission. The point source 2MASS J19142564+1109283 is indicated and contours of the radio continuum emission at 6 cm are included with levels of 5, 20, and $50\ \text{mJy beam}^{-1}$.

The broad *H*-band emission obtained with Gemini-NIRI towards G45.47 is presented in the left panel of Fig. 2, while the right panel displays the broad *K_s*-band emission of the same field. Both images were slightly smoothed to better display the diffuse emission that appears at the center of each panel and eastwards the point source 2MASS J19142564+1109283. This IR source was suggested to be an early B-type YSO by Ortega et al. (2012). The diffuse emission, better appreciated at the *K_s*-band, shows a nebula with a cone-like shape displaced $\sim 3''$ northwards the peak of the radio continuum emission at 6 cm, which is displayed with contours. The radio continuum data was extracted from the RMS Survey (Urquhart et al. 2009) and have a synthesized beam size of about $1''.7$. This displacement was previously found by De Buizer et al. (2005), who used mid-IR data with a resolution $> 1''.2$, and they could not fully discard an astrometric problem. Our observations confirm that the near-IR structure does not coincide with the radio continuum emission, evidencing the complexity of this massive star-forming region. Thus, as a first important result, we conclude that the UCH_{II} region G45.47 is not directly related to 2MASS J19142564+1109283 and its associated near-IR nebula. This is a similar case as found towards the hot molecular core G9.62+0.19, where some UCH_{II} regions, bright in radio continuum, have not any counterpart in near-IR (Linz et al. 2005). It seems to be common to find secondary cores slightly separated from UCH_{II} regions (e.g. Beuther et al. 2007).

Figure 3 shows a zoom-in of the *K_s*-band image with some emission contours to better display the morphology. The cone-like nebula, with an opening angle of about 90° , presents arc-like features with concave faces pointing to the IR source. These features seem to be connected to the IR source by a jet-like structure aligned with the blue shifted CO outflow found by Ortega et al. (2012). Figure 4 presents the *K_s*-band emission with contours displaying the blueshifted $^{12}\text{CO}\ J=3-2$ outflow and the $4.5\ \mu\text{m}$ IRAC emission. In the image, the blue arrow indicates the mentioned alignment. Thus, we suggest that the CO outflows are not related to the UCH_{II} region G45.47. The driving source of the outflows should be 2MASS J19142564+11092832.

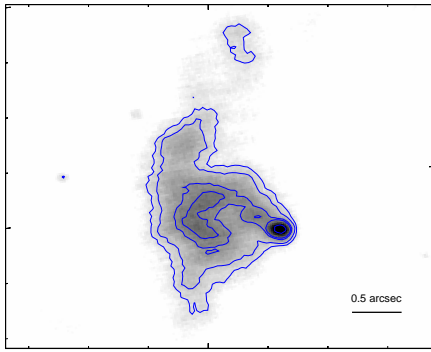


Fig. 3. Zoom-in of the *Ks*-band emission showing the cone-like shape nebula. Contours were included to better appreciate the morphology.

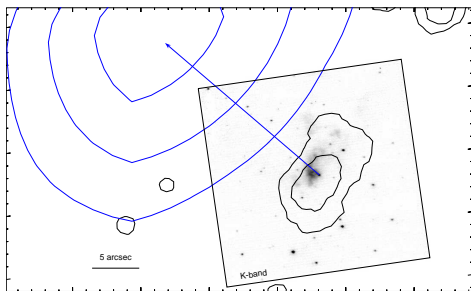


Fig. 4. The box shows the field observed with Gemini-NIRI and displays the broad *Ks*-band emission. The blue contours are the blueshifted CO outflow found by Ortega et al. (2012) and the black ones represent the $4.5 \mu\text{m}$ IRAC emission delimiting the EGO G45.47+0.05 boundaries. The angular resolution of the CO emission is about $20''$. The blue arrow shows the alignment between the structure that connects the IR source with the near-IR arc-like features and the blueshifted CO outflow.

The wide-angle ($\sim 90^\circ$) of the cone-like shape nebulosity pointing to the blue-shifted molecular outflow strongly suggests that the IR emission arises from a cavity cleared in the circumstellar material. The diffuse nebulosity seen at the *Ks*-band may be due to a combination of different emitting processes: continuum emission from the central protostar that is scattered at the inner walls of a cavity, emission from warm dust, and likely line emission from shock-excited H_2 , among other emission lines (e.g. Bik et al. 2006). The *H*-band emission shown in Fig. 2 (left), which presents a similar morphology as the *Ks*-band image, may also arise from scattered light and warm dust, and additionally from excited [FeII], tracer of the innermost part of jets that are accelerated near the driving source (Reipurth et al. 2000). It is important to note that we do not detect any similar feature related to the red-shifted molecular outflow detected by Ortega et al. (2012). This may be due to that the red-shifted component should be much fainter than the blue-shifted one because it is pointing away from us, which implies a higher extinction. Several studies show similar nebulosities related to MYSOs which are associated only with the blue-shifted outflow cavity (e.g. Preibisch et al. 2003; Kraus et al. 2006; Weigelt et al. 2006).

An outstanding unsolved problem concerning to jet-driven outflow models is how highly collimated jets can produce the wide-angle outflow cavities that are usually observed in massive protostellar envelopes (Mundt et al. 1990; Konigl & Pudritz 2000). Two possible scenarios have been proposed to explain this. One of them proposes a wide-angle structure produced

by the winds of the YSO with a density enhancement along the axis exhibiting a collimated jet-like appearance (Shu et al. 1995; Reipurth & Bally 2001). Weigelt et al. (2006) found that the cavity opening angle increases with increasing luminosity of the central source, supporting the hypothesis that a wide-angle stellar wind plays an important role in driving the outflows. In the second scenario, the wide-angle cavities are proposed to be excavated by the action of collimated precessing jets. Kraus et al. (2006) suggest that a precessing jet might explain the difference between the outflows widths observed towards low- and high-mass YSOs, adding support to a common collimation mechanism. According to the authors, the precession of a jet may be produced in a binary system where the rotational axis of the jet-driving star is misaligned with the orbital plane of its companion, or may be due to anisotropic accretion events that alters the angular momentum vector of the protostar disk.

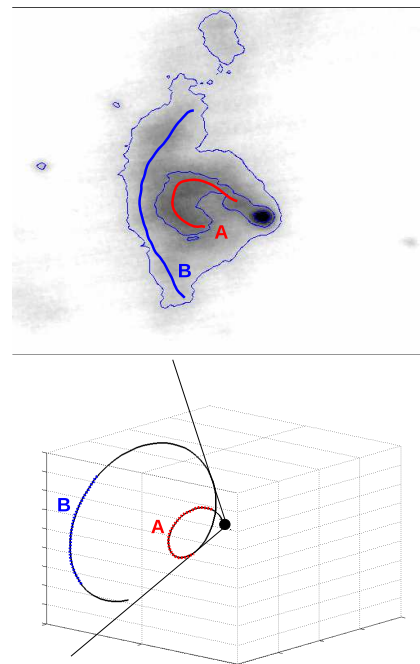


Fig. 5. Up: *Ks*-band emission towards G45.47. Some contours are superimposed and two arc-like features are remarked in red (feature A) and blue (feature B). Bottom: sketch of a likely scenario: a precessing jet coming to us describing an anticlockwise helicoid. The observed arc-like features A and B are remarked.

The wide-angle stellar wind and precessing jets models predict different geometries, which can be observationally distinguished. In the former model, the collimated jet-like structure is seen along the flow axis and the emission of the nebulosity structures exhibits a highly axial symmetry. On the other hand, in the precessing jet model, as the jet is free to move through the cavity, it is expected to observe asymmetries between the jet position and the emission from the nebulosity. In our observations, the most prominent arc-like structure (named A in Fig 5-up) is connected to the IR source through an elongated feature that may trace the most recently ejected material from the protostar. A clear asymmetry between the axis of the arc-like feature and the elongated feature is observed, which discards a wide-angle stellar wind scenario. A less conspicuous arc-like structure (the base of the cone-like structure; named B in Fig. 5-up) can be observed towards the east. This portion of the nebulosity is clumpy and its concavity points to the IR source as in the case of

feature A. Thus, the morphology of the observed nebula suggests an spiraling shape produced by a precessing jet. Moreover, the isolated fragment detected towards the north could be associated with the arc-like feature B, evidencing the asymmetric nature of the cavity and supporting the interpretation of a precessing jet. In Fig. 5-bottom we show the arc-like features named A and B in an sketch of an anticlockwise helicoid, with an angle of 50° respect to the plane of the sky. Following the models presented in Smith & Rosen (2005), who state that the dominant physical structure for all precessing jets is an inward-facing cone, we suggest that the arc-like morphology observed in our *Ks*-band image is consistent with a slow precessing jet. Smith & Rosen (2005) show that a fast-precessing jet (precession period = 50 yr) rapidly disrupts into many bow shocks, while a slow-precessing jet (precession period = 400 yr) leads to helical flows generating an spiraling shape nebula. Following the authors, the observed fragmented helicoid structure in our *Ks*-band image can obey to the pulsating intrinsic nature of the precessing jet or to inhomogeneities of the circumstellar material.

Binary systems can be found in different stellar evolution stages. For example, Connelley et al. (2008) found that for Class I YSOs, the binary frequency of systems with separations between 100 and 4500 A.U. is about 43%. Chini et al. (2012) show a high binarity statistics for O- and B-type stars. As previously mentioned, in binary protostars systems with misaligned disk, a jet precession is expected due to the tidal interactions between companions (e.g. Papaloizou & Terquem 1995). Using the relation given in Bate et al. (2000), $P_{prec} \sim 20 \times P_{bin}$, where P_{prec} and P_{bin} are the precession and the binary orbital periods, respectively, and assuming a slow precessing period of 400 yrs, a $P_{bin} \sim 20$ yrs is derived. From the generalization of Kepler's third law (see eq. 12.15 from Stahler & Palla 2005) and considering a relatively large binary system mass of $50 M_\odot$ we derive a maximum separation of 27 A.U. between the system components. With the angular resolution in our image of $0''.15$ (1200 A.U. at a distance of 8 kpc) we could not spatially resolve any possible binarity under these assumptions. Furthermore, we can not discard the presence of deeply embedded sources not detected at near-IR, whose existence could be revealed at longer wavelengths (see Linz et al. 2005). Thus, we conclude that binary-induced jet precession may be a plausible scenario. However, we can not rule out the anisotropic accretion events as the responsible of the jet precession. Spectroscopic observations are required to discern between both scenarios.

4. Summary

Using the NIRI instrument at the Gemini North Telescope and the adaptative optic system ALTAIR we studied the near-IR emission from the UCHII region G045.47+0.05, a massive star forming site located at a distance of about 8 kpc. Achieving an angular resolution of $0''.15$ we obtained *H*- and *Ks*-band images with a great level of detail, which allowed us to unveil the driven mechanism of the massive molecular outflows found in a previous study.

We found near-IR diffuse emission with a cone-like shape extending eastwards the IR source 2MASS J19142564+1109283, a very likely MYSO. This morphology suggests a cavity that was cleared in the circumstellar material and its emission may arise from a combination of different emitting processes: continuum emission from the central protostar that is scattered at the inner walls of a cavity, emission from warm dust, and likely emission lines from shock-excited gas. The cone-like nebula, with an opening angle of about 90° ,

presents some arc-like features whose concave faces point to the IR source. These features seem to be connected to the IR source by a jet-like structure aligned with the blue shifted CO outflow found in a previous study. The near-IR structure lies $\sim 3''$ north of the radio continuum emission, revealing that it is not spatially coincident with the UCHII region and strongly suggesting that the outflows are not generated by it. The driving source of the outflows should be 2MASS J19142564+1109283. Taking into account the observed asymmetry between the axis of the arc-like features and the elongated structure that connects them to the IR source, we propose that the spiraling shape of the nebula is produced by a precessing jet. The observed fragmented helicoid structure may be due to the pulsating intrinsic nature of the precessing jet or to inhomogeneities of the circumstellar material. We propose that the jet precession may be due to tidal interactions in an unresolved binary system or to anisotropic accretion events occurring in one MYSO. Spectroscopic observations are required to discern between both scenarios. In any case, we conclude that we are resolving the circumstellar ambient of a distant (6-9 kpc) MYSO, indeed one of the farthest cases.

Acknowledgements. We would like to thank the anonymous referee for her/his extremely helpful comments. S.P. and M.O. are members of the *Carrera del investigador científico* of CONICET, Argentina. This work was partially supported by grants awarded by CONICET, ANPCYT and UBA (UBACyT).

References

- Araya, E., Hofner, P., Churchwell, E., & Kurtz, S. 2002, *ApJS*, 138, 63
 Bate, M. R., Bonnell, I. A., Clarke, C. J., et al. 2000, *MNRAS*, 317, 773
 Benjamin, R. A., Churchwell, E., Babler, B. L., et al. 2003, *PASP*, 115, 953
 Beuther, H., Zhang, Q., Bergin, E. A., et al. 2007, *A&A*, 468, 1045
 Bik, A., Kaper, L., & Waters, L. B. F. M. 2006, *A&A*, 455, 561
 Boccas, M., Rigaut, F., Bec, M., et al. 2006, in *Society of Photo-Optical Instrumentation Engineers (SPIE) Conference Series*, Vol. 6272
 Caswell, J. L., Vaile, R. A., Ellingsen, S. P., Whiteoak, J. B., & Norris, R. P. 1995, *MNRAS*, 272, 96
 Cesaroni, R., Walmsley, C. M., & Churchwell, E. 1992, *A&A*, 256, 618
 Chini, R., Hoffmeister, V. H., Nasser, A., Stahl, O., & Zinnecker, H. 2012, *MNRAS*, 424, 1925
 Connelley, M. S., Reipurth, B., & Tokunaga, A. T. 2008, *AJ*, 135, 2496
 Cyganowski, C. J., Whitney, B. A., Holden, E., et al. 2008, *AJ*, 136, 2391
 De Buizer, J. M., Radomski, J. T., Telesco, C. M., & Piña, R. K. 2005, *ApJS*, 156, 179
 Herriot, G., Morris, S., Anthony, A., et al. 2000, in *Society of Photo-Optical Instrumentation Engineers (SPIE) Conference Series*, ed. P. L. Wizinowich, Vol. 4007, 115–125
 Hester, J. J. & Desch, S. J. 2005, in *Astronomical Society of the Pacific Conference Series*, Vol. 341, *Chondrites and the Protoplanetary Disk*, ed. A. N. Krot, E. R. D. Scott, & B. Reipurth, 107
 Hodapp, K. W., Jensen, J. B., Irwin, E. M., et al. 2003, *PASP*, 115, 1388
 Hunter, T. R., Phillips, T. G., & Menten, K. M. 1997, *ApJ*, 478, 283
 Konigl, A. & Pudritz, R. E. 2000, *Protostars and Planets IV*, 759
 Kraus, S., Balega, Y., Elitzur, M., et al. 2006, *A&A*, 455, 521
 Kuchar, T. A. & Bania, T. M. 1994, *ApJ*, 436, 117
 Linz, H., Stecklum, B., Henning, T., Hofner, P., & Brandl, B. 2005, *A&A*, 429, 903
 Mundt, R., Buehrke, T., Solf, J., Ray, T. P., & Raga, A. C. 1990, *A&A*, 232, 37
 Ortega, M. E., Paron, S., Cichowolski, S., Rubio, M., & Dubner, G. 2012, *A&A*, 546, A96
 Papaloizou, J. C. B. & Terquem, C. 1995, *MNRAS*, 274, 987
 Paron, S., Cichowolski, S., & Ortega, M. E. 2009, *A&A*, 506, 789
 Peters, T., Banerjee, R., Klessen, R. S., et al. 2010, *ApJ*, 711, 1017
 Preibisch, T., Balega, Y. Y., Schertl, D., & Weigelt, G. 2003, *A&A*, 412, 735
 Qin, S.-L., Wang, J.-J., Zhao, G., Miller, M., & Zhao, J.-H. 2008, *A&A*, 484, 361
 Reipurth, B. & Bally, J. 2001, *ARA&A*, 39, 403
 Reipurth, B., Yu, K. C., Heathcote, S., Bally, J., & Rodríguez, L. F. 2000, *AJ*, 120, 1449
 Shu, F. H., Najita, J., Ostriker, E. C., & Shang, H. 1995, *ApJ*, 455, L155
 Smith, M. D. & Rosen, A. 2005, *MNRAS*, 357, 579
 Stahler, S. W. & Palla, F. 2005, *The Formation of Stars*, ISBN 3-527-40559-3, Wiley-VCH
 Urquhart, J. S., Hoare, M. G., Purcell, C. R., et al. 2009, *A&A*, 501, 539
 Vaidya, B., Fendt, C., Beuther, H., & Porth, O. 2011, *ApJ*, 742, 56
 Weigelt, G., Beuther, H., Hofmann, K.-H., et al. 2006, *A&A*, 447, 655
 Wilner, D. J., Ho, P. T. P., & Zhang, Q. 1996, *ApJ*, 462, 339
 Wood, D. O. S. & Churchwell, E. 1989, *ApJS*, 69, 831
 Wu, Y., Wei, Y., Zhao, M., et al. 2004, *A&A*, 426, 503